MOLECULAR GENETICS

# Enhanced CRISPR-Cas9 correction of Duchenne muscular dystrophy in mice by a self-complementary AAV delivery system

Yu Zhang[1,2], Hui Li[1,2], Yi-Li Min[1,2]*, Efrain Sanchez-Ortiz[1,2], Jian Huang[3], Alex A. Mireault[1,2], John M. Shelton[3], Jiwoong Kim[4], Pradeep P. A. Mammen[2,3], Rhonda Bassel-Duby[1,2], Eric N. Olson[1,2]†



**Duchenne muscular dystrophy (DMD) is a lethal neuromuscular disease caused by mutations in the dystrophin gene (*DMD*). Previously, we applied CRISPR-Cas9–mediated "single-cut" genome editing to correct diverse genetic mutations in animal models of DMD. However, high doses of adeno-associated virus (AAV) are required for efficient in vivo genome editing, posing challenges for clinical application. In this study, we packaged Cas9 nuclease in single-stranded AAV (ssAAV) and CRISPR single guide RNAs in self-complementary AAV (scAAV) and delivered this dual AAV system into a mouse model of DMD. The dose of scAAV required for efficient genome editing were at least 20-fold lower than with ssAAV. Mice receiving systemic treatment showed restoration of dystrophin expression and improved muscle contractility. These findings show that the efficiency of CRISPR-Cas9–mediated genome editing can be substantially improved by using the scAAV system. This represents an important advancement toward therapeutic translation of genome editing for DMD.**

## INTRODUCTION

Duchenne muscular dystrophy (DMD) is an X-linked monogenic neuromuscular disease caused by mutations in the *DMD* gene, which encodes dystrophin (*1*, *2*). Dystrophin, together with dystroglycans and sarcoglycans, maintains sarcolemma integrity and stability by interacting with intracellular actin and extracellular laminin (*3*–*5*). More than 4000 mutations have been identified in patients with DMD, including single- and multiexon deletions or duplications and small missense or nonsense substitutions (*6*, *7*). Patients with DMD manifest progressive muscle weakness and ultimately develop fatal respiratory and cardiac failure in their mid-20s.

To date, two clinical therapies are available for DMD treatment, including steroid supplementation and morpholino antisense oligomer injection (*8*, *9*). Long-term corticosteroid supplement partially alleviates DMD pathological phenotypes but cannot restore dystrophin expression. Morpholino antisense oligomers allow skipping of mutant *DMD* exons, but less than 1% of normal levels of dystrophin protein can be restored by this treatment (*9*). In addition, several clinical trials are currently evaluating the therapeutic benefits of truncated versions of dystrophin delivered by adeno-associated virus (AAV) (*10*). However, these gene replacement therapies cannot restore the expression of endogenous dystrophin protein and are dependent on the expression pattern of the exogenous promoters within the AAV, as well as the longevity of AAV expression. Thus, developing a strategy for permanent and efficient correction of mutations in the endogenous *DMD* gene may provide an ultimate cure for this lethal neuromuscular disorder.

Application of the CRISPR-Cas (clustered regularly interspaced short palindromic repeats and CRISPR-associated proteins) system for engineering site-specific DNA double-stranded breaks (DSBs) provides simplicity and precision in mammalian genome editing (*11*–*13*). We and others showed that the CRISPR-Cas system can be used to efficiently correct missense mutations in mouse models of DMD by homology-directed repair–based germline editing or nonhomologous end joining (NHEJ)–based postnatal editing (*14*–*22*). While missense and nonsense substitutions only account for ~20% of *DMD* mutations, single- or multiexon deletions are more prevalent (~68%) in DMD populations (*6*, *7*). We recently reported the successful rescue of DMD phenotypes in mice and dogs harboring exon 44 or 50 deletions by injecting recombinant AAV9-packaged Cas9 nuclease and single guide RNAs (sgRNAs) (*23*–*25*). These studies demonstrated that the CRISPR-Cas system can be deployed to correct diverse genetic mutations that cause DMD and offer the prospect of a potential gene therapy for the permanent correction of DMD.

Currently, the most widely used delivery vector for gene therapy is recombinant AAV, which is a non-enveloped virus with a single-stranded linear DNA viral genome (*26*). As the largest tissue in the human body, skeletal muscle accounts for ~40% of body weight. Therefore, a high dose of AAV [$5.5 \times 10^{14}$ to $1.8 \times 10^{15}$ vector genomes (vg)/kg] is required to achieve long-term, efficient genome editing in animal models of DMD (*20*–*22*, *25*). However, several studies in large animals reported that systemic administration of high doses of AAV ($\geq 1.5 \times 10^{14}$ vg/kg) may cause acute liver toxicity (*27*, *28*). In addition, in our previous study, we found that the efficiency of in vivo CRISPR-Cas9–mediated genome editing was highly dose dependent and that elevating the dose of sgRNA AAV relative to Cas9 AAV enhanced the efficiency of genome editing (*25*). Moreover, it has been suggested that the sgRNA AAV genome is preferentially depleted after systemic delivery of CRISPR-Cas9 genome editing components (*21*). Therefore, systemic delivery of CRISPR-Cas9 genome editing components by a high dose of single-stranded AAV (ssAAV) for the treatment of DMD remains challenging.

To reduce the viral dose used for gene therapy without compromising genome editing efficiency and to prevent preferential depletion of the sgRNA AAV genome, we packaged a CRISPR sgRNA expression cassette into a double-stranded AAV vector. A double-stranded AAV

[1]Department of Molecular Biology, University of Texas Southwestern Medical Center, Dallas, TX 75390, USA. [2]Senator Paul D. Wellstone Muscular Dystrophy Cooperative Research Center, University of Texas Southwestern Medical Center, Dallas, TX 75390, USA. [3]Department of Internal Medicine, University of Texas Southwestern Medical Center, Dallas, TX 75390, USA. [4]Department of Population and Data Sciences, University of Texas Southwestern Medical Center, Dallas, TX 75390, USA.
*Present address: Exonics Therapeutics, 490 Arsenal Way, Watertown, MA 02472, USA.
†Corresponding author. Email: eric.olson@utsouthwestern.edu

genome can be generated by mutating the terminal resolution site sequence on one side of the inverted terminal repeats (ITR), leading to production of self-complementary AAV (scAAV) (*29*, *30*). Unlike conventional ssAAV, scAAV can bypass the second-strand synthesis, which is a rate-limiting step for gene expression (*31*, *32*). Moreover, double-stranded scAAV is less prone to DNA degradation after viral transduction, thereby increasing the number of copies of stable episomes (*33*, *34*). The scAAV system has been used in several gene replacement clinical trials for the treatment of spinal muscular atrophy and limb-girdle muscular dystrophy (*35*, *36*).

In this study, we performed in vivo genome editing in mice with a deletion of *Dmd* exon 44 (ΔEx44) by coupling ssAAV-packaged *Sp*Cas9 nuclease with scAAV-expressed sgRNAs. This dual AAV delivery system provided substantial improvements in viral transduction efficiency, genome editing, and functional recovery in skeletal muscles and heart. Notably, at least 20-fold less scAAV was required to achieve these improvements compared to the ssAAV-treated cohort. Thus, the scAAV system represents a promising strategy for delivering CRISPR-Cas9 genome editing components and represents an important advancement toward potential therapeutic translation.

## RESULTS

### Strategies for CRISPR-Cas9–mediated genome editing of *Dmd* exon 45

Deletion of exon 44 of the human *DMD* gene generates a premature stop codon in exon 45 and represents one of the most common mutations of DMD. As a strategy to correct exon 44 out-of-frame deletion mutations, we designed an sgRNA to target the splice acceptor region of exon 45 (Fig. 1A). This sgRNA recognizes a 5′-TGG-3′ protospacer adjacent motif (PAM) in exon 45 and generates insertions and deletions (INDELs) 7 base pairs downstream of the 5′-AG-3′ splice acceptor site (Fig. 1B). Depending on the size of INDELs, two types of NHEJ-mediated DNA repair events can restore the open reading frame (ORF) of the *Dmd* gene. These include exon 45 skipping, if the INDEL is large enough to delete the 5′-AG-3′ splice acceptor sequence in exon 45, or reframing of exon 45 through INDELs that either insert one nucleotide (3n + 1) or delete two nucleotides (3n − 2) (Fig. 1A).

To test whether double-stranded scAAV is capable of packaging sgRNAs, we cloned the sgRNA expression cassette into an scAAV vector and the conventional ssAAV vector as a control (Fig. 1C). Alkaline denaturing gel electrophoresis was performed to confirm the integrity of both AAVs (fig. S1). The size of ssAAV-sgRNA is 3.9 kilonucleotides (knt) and remains unchanged after alkaline gel electrophoresis. The size of scAAV-sgRNA is 1.4 kilo–base pairs and is doubled to 2.8 knt under denaturing conditions, indicative of the double-stranded viral genome.

### In vitro genome editing using ssAAV or scAAV-packaged sgRNA

To compare the efficiency of ssAAV- and scAAV-packaged sgRNAs in vitro, we differentiated *Sp*Cas9-expressing C2C12 mouse myoblasts for 5 days to myotubes and transduced the myotubes with each of the AAVs. One week after viral transduction, we performed tracking of INDELs by decomposition (TIDE) analysis to detect INDELs within the *Dmd* exon 45 region. We found that the total INDELs exhibited a dose-dependent curve for both ssAAV- and scAAV-expressed sgRNA 1 week after viral transduction (Fig. 1D). Specifically, to reach a 10% level of INDELs, scAAV ($5 \times 10^8$ vg/ml) and ssAAV ($1 \times 10^{10}$ vg/ml) were required, representing a 20-fold increase in efficiency of scAAV. To reach an intermediate level of INDELs of ~22%, 40-fold less scAAV ($1.8 \times 10^9$ vg/ml) was required compared to ssAAV ($7.8 \times 10^{10}$ vg/ml). Furthermore, a high level of INDELs (over 40%) was achieved by scAAV ($7.2 \times 10^9$ vg/ml), whereas ssAAV required $5 \times 10^{12}$ vg/ml, representing a 70-fold improvement in efficiency with scAAV. We also analyzed the INDEL composition in myotubes transduced with ssAAV or scAAV and found that ~50% of total INDEL events contained a +1-nt insertion, which can bring exon 45 in-frame with exon 43 (Fig. 1E). Therefore, scAAV-expressed sgRNA demonstrated enhanced efficiency by in vitro genome editing at *Dmd* exon 45 compared to the conventional ssAAV-expressed sgRNA. Moreover, the majority of the INDEL events (more than 50%) contained a single nucleotide insertion, which is able to restore the *Dmd* exon 45 ORF.

### Systemic delivery of scAAV-packaged sgRNAs restores dystrophin expression in ΔEx44 mice

To further evaluate the efficacy of the scAAV system by in vivo genome editing, we delivered ssAAV-packaged *Sp*Cas9 and scAAV- or ssAAV-packaged sgRNA systemically in ΔEx44 mice through intraperitoneal injection. The AAV9 serotype was chosen because of its tropism to skeletal muscle and heart (*37*). Moreover, *Sp*Cas9 expression was driven by a muscle-specific promoter containing key regulatory elements derived from creatine kinase (CK) promoter and enhancer, restricting its expression to striated muscles (*38*). Recent studies demonstrate that AAV-packaged sgRNA is the rate-limiting factor for in vivo genome editing in dystrophic mouse models (*21*, *25*). Therefore, we kept ssAAV-packaged *Sp*Cas9 at a constant dose of $8 \times 10^{13}$ vg/kg while titrating scAAV- or ssAAV-packaged sgRNA at multiple doses. Four weeks after systemic AAV delivery, the skeletal muscles and heart of CRISPR-Cas9–edited ΔEx44 mice were harvested for analysis. By immunohistochemistry, we found that dystrophin restoration in skeletal muscles was dose dependent (Fig. 2 and fig. S2). Mice receiving the lowest dose of scAAV-packaged sgRNA ($4 \times 10^{12}$ vg/kg) showed 40 and 32% dystrophin-positive myofibers in the tibialis anterior (TA) and triceps, respectively; the diaphragm and heart showed higher percentages of dystrophin-positive myocytes, reaching 95% (Fig. 2 and fig. S3A). In contrast to the scAAV-treated cohort, ΔEx44 mice receiving the lowest dose of ssAAV-packaged sgRNA ($4 \times 10^{12}$ vg/kg) showed less than 5% dystrophin-positive myofibers in the TA and triceps; the diaphragm and heart showed 52 and 61% dystrophin-positive myocytes, respectively (figs. S2 and S3B). When the dose of scAAV-packaged sgRNA was increased to $1.6 \times 10^{13}$ vg/kg, virtually all myofibers and cardiomyocytes were dystrophin positive (Fig. 2 and fig. S3A). For the ssAAV-treated cohort ($1.6 \times 10^{13}$ vg/kg), the diaphragm and heart showed more than 75% of dystrophin-positive myocytes; however, dystrophin-positive myofibers in the TA and triceps were still below 18% (figs. S2 and S3B).

Next, we performed Western blot analysis to quantitatively detect dystrophin restoration in skeletal muscles and heart after systematic delivery of scAAV- or ssAAV-packaged sgRNA. The lowest dose of scAAV-packaged sgRNA ($4 \times 10^{12}$ vg/kg) restored 18, 14, and 50% of dystrophin protein in the TA, triceps, and diaphragm, respectively (Fig. 3, A and B). When the dose of scAAV-packaged sgRNA was increased to $1.6 \times 10^{13}$ vg/kg, dystrophin protein restoration in each skeletal muscle group was greater than 50% (Fig. 3, A and B). Notably, saturation was observed in the heart because at every dose of scAAV tested, dystrophin protein restoration exceeded 70% (Fig. 3, A and B).

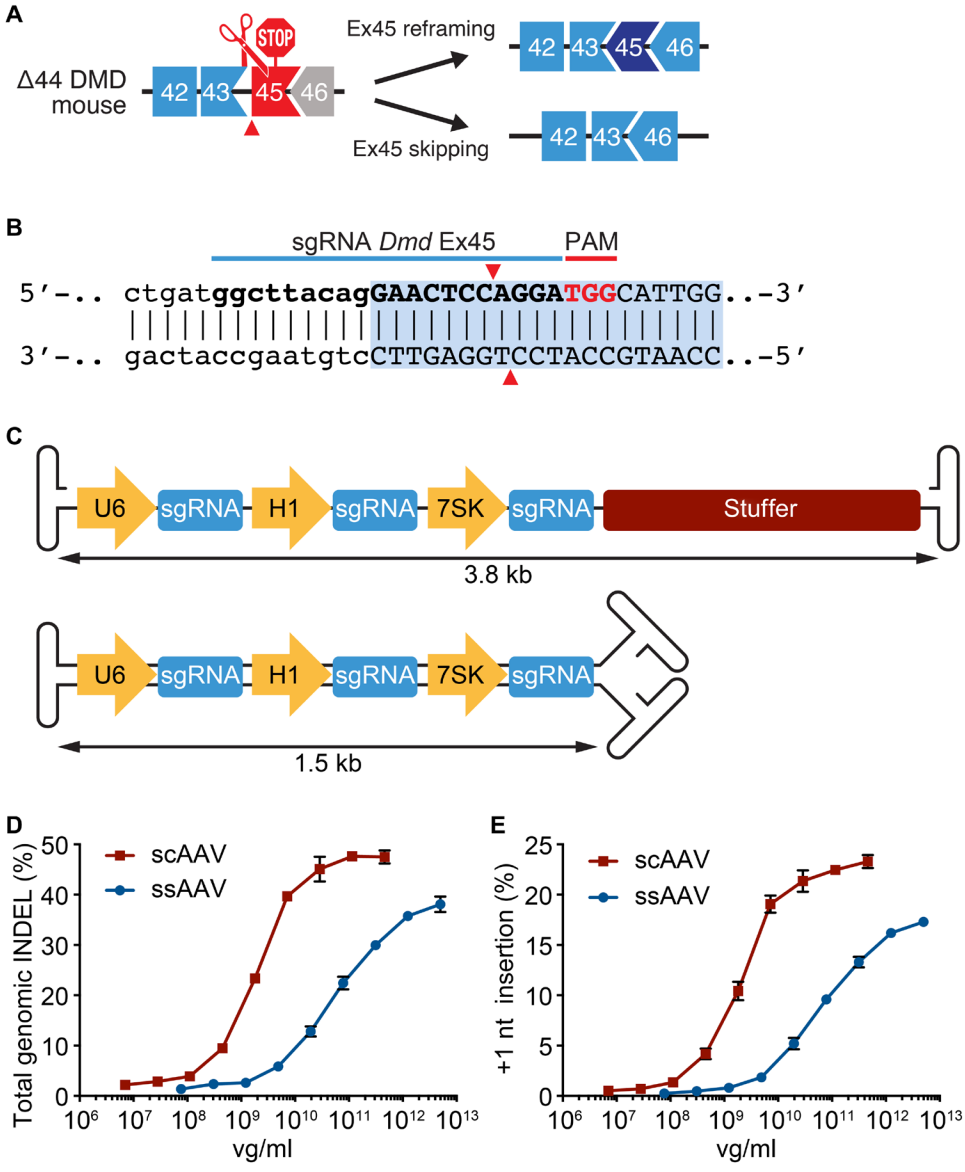


**Fig. 1. Strategies for CRISPR-Cas9–mediated genome editing in *Dmd* ΔEx44 mice.** (**A**) An out-of-frame deletion of *Dmd* exon 44 results in splicing of exons 43 to 45, generating a premature stop codon in exon 45. A CRISPR-Cas9–mediated "single-cut" strategy was designed to restore the open reading frame (ORF) of the *Dmd* gene. If the genomic insertions and deletions (INDELs) result in one nucleotide insertion (3n + 1) or two nucleotide deletion (3n − 2), then exon 45 will be reframed with adjacent exons 43 and 46. If the INDEL is large enough to delete the 5′-AG-3′ splice acceptor sequence, then exon 45 will be skipped, resulting in splicing of exon 43 to exon 46. (**B**) Illustration of sgRNA targeting *Dmd* exon 45. This sgRNA recognizes a 5′-TGG-3′ PAM in exon 45 and generates a cut 7 base pairs downstream of the 5′-AG-3′ splice acceptor site. (**C**) Illustration of AAV vectors used to deliver the sgRNA expression cassette. Three copies of the same sgRNA are driven by three RNA polymerase III promoters, U6, H1, and 7SK. The top vector produces ssAAV. A 2.3-kb stuffer sequence was cloned into the ssAAV vector for optimal packaging. The bottom vector produces double-stranded scAAV. (**D**) Analysis of total INDEL event in 5-day differentiated myotubes transduced with scAAV- or ssAAV-packaged sgRNA at multiple doses. Data are presented as mean ± SEM ($n = 3$). (**E**) Analysis of the +1-nt insertion event in 5-day differentiated myotubes transduced with scAAV- or ssAAV-packaged sgRNA at multiple doses. Data are presented as mean ± SEM ($n = 3$).

Although ssAAV-packaged *Sp*Cas9 was injected at a constant dose ($8 \times 10^{13}$ vg/kg), ΔEx44 mice receiving a higher dose of scAAV-packaged sgRNA showed elevated Cas9 protein expression in skeletal muscles and heart (Fig. 3, A and C), which is consistent with our previous publication when dosing ssAAV-packaged sgRNA (*25*). In contrast to the scAAV-treated cohort, ΔEx44 mice receiving ssAAV-packaged sgRNA showed significantly lower efficiency in dystrophin restoration by Western blot quantification (fig. S4). Specifically, mice receiving the highest dose of ssAAV ($8 \times 10^{13}$ vg/kg) showed only 13, 16, and 30% of normal dystrophin protein levels in the TA, triceps, and diaphragm, respectively (fig. S4). This was incomparable to the mice treated with scAAV because more than 80% of dystrophin protein was restored after receiving the same dose of scAAV-packaged sgRNA (Fig. 3, A and B). Therefore, scAAV-expressed sgRNA demonstrated greater efficiency in in vivo genome editing compared to the conventional ssAAV-expressed sgRNA.

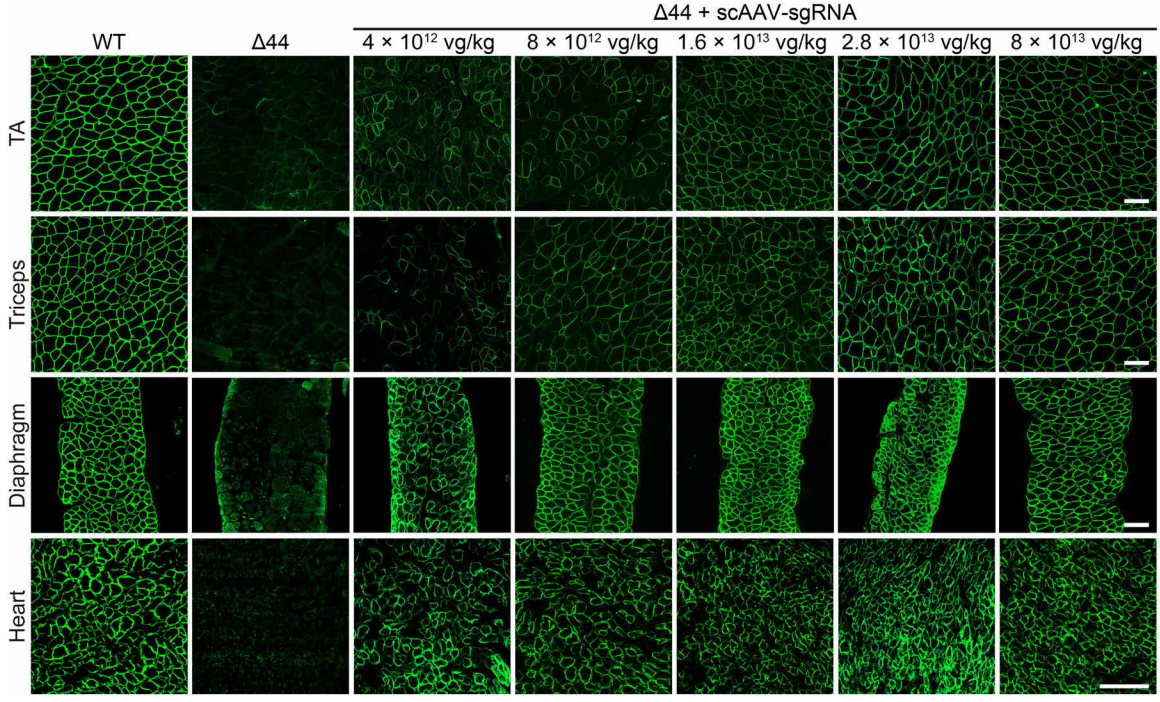


**Fig. 2. Systemic AAV delivery of CRISPR-Cas9 genome editing components to ΔEx44 mice rescues dystrophin expression.** Immunohistochemistry shows restoration of dystrophin in the tibialis anterior (TA), triceps, diaphragm, and heart of ΔEx44 mice 4 weeks after systemic delivery of ssAAV-packaged *Sp*Cas9 and scAAV-packaged sgRNA. The *Sp*Cas9 vector was kept at a constant dose of $8 \times 10^{13}$ vg/kg. The dose of the sgRNA vector is shown in the figure. Dystrophin is shown in green. $n = 5$ for each muscle group. Scale bars, 100 μm.

### Systemic delivery of scAAV-packaged sgRNAs restores muscle integrity and improves muscle function in ΔEx44 mice

To evaluate whether systemic delivery of scAAV-packaged sgRNAs was able to rescue pathological hallmarks seen in dystrophic mice, we performed hematoxylin and eosin (H&E) staining of skeletal muscles and heart isolated from ΔEx44 mice 4 weeks after CRISPR-Cas9–mediated genome editing. The percentage of regenerating myofibers with central nuclei declined, as the dose of scAAV-packaged sgRNA increased (figs. S5 and S6). Less than 5% of myofibers showed central nuclei in the TA and triceps in mice receiving scAAV-packaged sgRNA ($1.6 \times 10^{13}$ vg/kg) (figs. S5A and S6A). In contrast, mice receiving the same dose of ssAAV-packaged sgRNA still showed more than 70% of regenerating myofibers with central nuclei, together with signs of muscle necrosis and inflammatory infiltration (figs. S5B and S6B). In addition, skeletal muscles isolated from mice receiving the highest dose of scAAV-packaged sgRNA ($8 \times 10^{13}$ vg/kg) were virtually indistinguishable from those of wild-type (WT) littermates, whereas the ssAAV-treated cohort still showed 30% central nuclei in the TA and triceps (figs. S5 and S6).

To examine the effect of dystrophin restoration on muscle function after systemic delivery of scAAV- or ssAAV-packaged sgRNA, we performed electrophysiological analyses on the extensor digitorum longus (EDL) and soleus muscles isolated from ΔEx44 mice 4 weeks after receiving the middle dose of AAV-sgRNA ($1.6 \times 10^{13}$ vg/kg) or the high dose of AAV-sgRNA ($8 \times 10^{13}$ vg/kg). Without CRISPR-Cas9 genome editing, muscle-specific force, which was calibrated by the muscle cross-sectional area, was reduced by 46% in fast-twitch EDL muscle and by 42% in slow-twitch soleus muscle (Fig. 4, A and B). After systemic delivery of scAAV-packaged sgRNA, muscle-specific force of the EDL was increased from 54 to 83% and to 82% for the middle and high doses, respectively; in contrast, for the ssAAV-treated cohort, muscle-specific force of the EDL was only increased from 54 to 62% and to 66% for the middle and high doses, respectively (Fig. 4A). For the slow-twitch soleus muscle, muscle-specific force was increased from 58 to 93% and to 96% after receiving the middle and high doses of scAAV-packaged sgRNA; in contrast, for the ssAAV-treated cohort, only high-dose treatment was able to improve muscle-specific force of the soleus to 85%, while no improvement was observed with the middle dose (Fig. 4B). The maximal tetanic force of the EDL and soleus followed a similar pattern to the muscle-specific force. Specifically, ΔEx44 mice receiving the middle or high doses of scAAV-packaged sgRNA showed improved maximal tetanic force of the EDL muscle to more than 80% of WT, whereas the ssAAV-treated cohort was only able to improve 60% of WT (Fig. 4C). The maximal tetanic force of the soleus was improved to more than 90% of WT after receiving the middle or high doses of scAAV-packaged sgRNA; the high dose of ssAAV-packaged sgRNA improved the maximal tetanic force of the soleus to 85% of WT, while the middle dose did not provide any improvement (Fig. 4D). After receiving the middle and high doses of scAAV-packaged sgRNA, serum CK levels in the ΔEx44 mice were reduced by 87 and 95%, respectively, compared with ΔEx44 mice without treatment (fig. S7). In contrast, serum CK levels in the ΔEx44 mice receiving the same doses of ssAAV-packaged sgRNA were still 18.6- and 8.5-fold higher, respectively, than the WT littermates (fig. S7). These findings indicate that the double-stranded scAAV vector is highly efficient in in vivo gene therapy and can substantially improve muscle integrity and function.

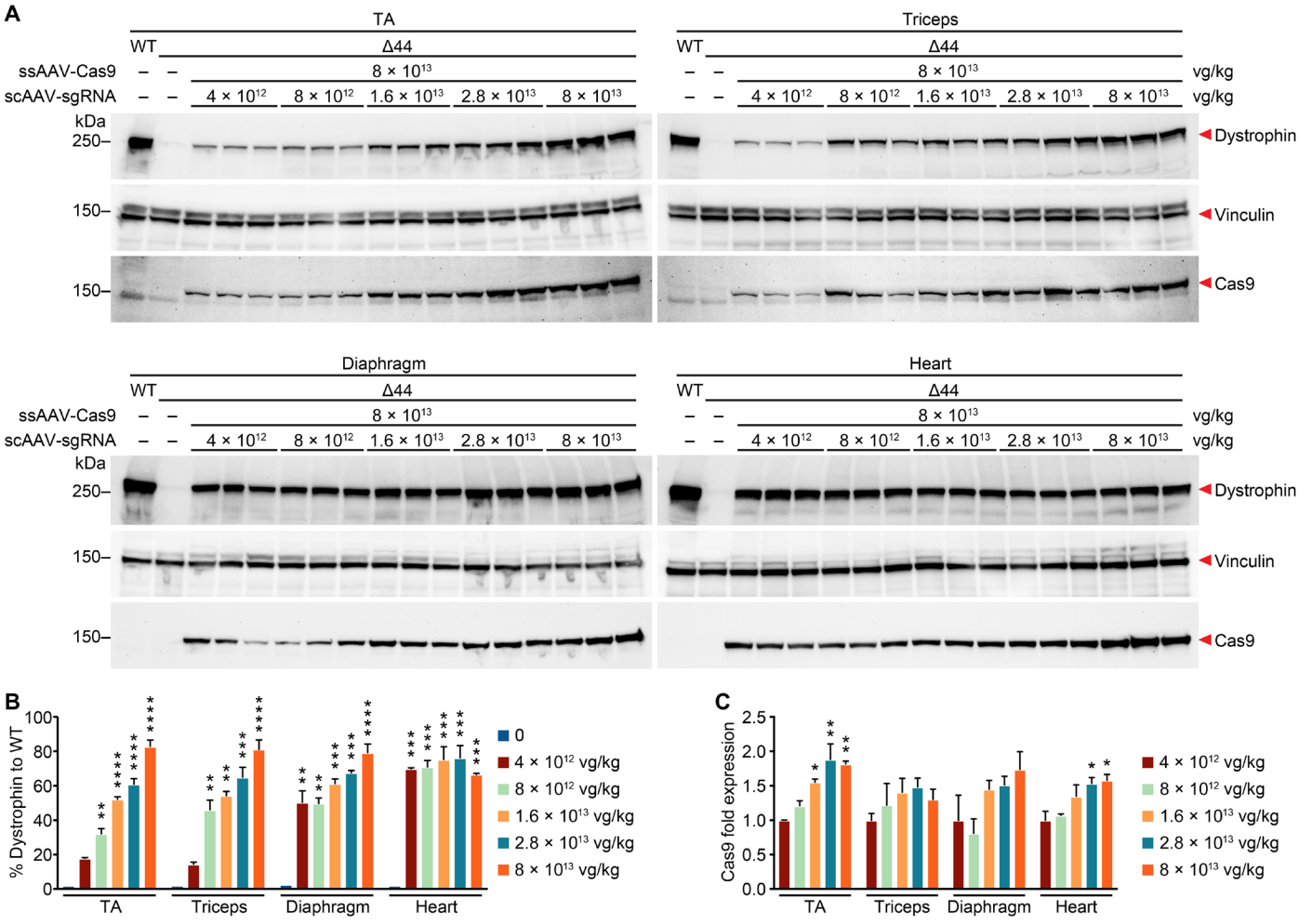


**Fig. 3. Western blot analysis of skeletal muscles and heart of ΔEx44 mice receiving systemic AAV delivery of CRISPR-Cas9 genome editing components.** (**A**) Western blot analysis shows restoration of dystrophin expression in the TA, triceps, diaphragm, and heart of ΔEx44 mice 4 weeks after systemic delivery of ssAAV-packaged *Sp*Cas9 and scAAV-packaged sgRNA. The *Sp*Cas9 vector was kept at a constant dose of $8 \times 10^{13}$ vg/kg. The dose of the sgRNA vector is shown in the figure. Vinculin was used as the loading control ($n = 3$). (**B**) Quantification of dystrophin expression in the TA, triceps, diaphragm, and heart. Relative dystrophin intensity was calibrated with vinculin internal control before normalizing to the WT control. Data are presented as mean ± SEM. One-way ANOVA was performed with post hoc Tukey's multiple comparisons test. $^{**}P < 0.005$, $^{***}P < 0.001$, $^{****}P < 0.0001$ ($n = 3$). (**C**) Quantification of Cas9 expression in the TA, triceps, diaphragm, and heart. Relative Cas9 intensity was calibrated with vinculin internal control before normalizing to the group treated with the lowest dose of scAAV-packaged sgRNA ($4 \times 10^{12}$ vg/kg). Data are presented as mean ± SEM. One-way ANOVA was performed with post hoc Tukey's multiple comparisons test. $^{*}P < 0.05$, $^{**}P < 0.005$ ($n = 3$).

## The scAAV system induces significant INDELs within *Dmd* exon 45 and maintains higher copies of the viral genome in vivo

To determine the mechanism whereby the scAAV system substantially improves in vivo genome editing in ΔEx44 mice, we performed deep sequencing analysis to determine the INDEL frequency at the genomic level (Fig. 5A and table S1). The percentage of total genomic INDELs and +1-nt insertions at exon 45 correlated with ascending doses of AAV-sgRNA. ΔEx44 mice receiving the high dose ($8 \times 10^{13}$ vg/kg) of scAAV-packaged sgRNA showed more than 28 and 30% of the total NHEJ events in the TA and triceps, respectively (Fig. 5A). Notably, more than 60% of the total NHEJ events were +1-nt insertions, which restores the *Dmd* exon 45 ORF. In contrast, the TA and triceps from ΔEx44 mice receiving the same dose of ssAAV-packaged sgRNA had only 10 and 11% of the total NHEJ events (Fig. 5A). We did not observe a significant difference between scAAV and ssAAV in inducing total NHEJ and +1-nt insertion events in the diaphragm or heart (Fig. 5A). We observed a low percentage of AAV integration events at the sgRNA targeting site in ssAAV- and scAAV-treated mice (table S1).

We also performed TIDE analysis on dystrophin cDNA transcripts isolated from skeletal muscles and heart. Total cDNA INDEL rate and +1-nt insertion events at exon 45 followed similar ascending patterns seen in the genomic deep sequencing analysis, while the absolute percentage increased significantly (Fig. 5B), indicating enrichment of the reframed cDNA transcript after nonsense-mediated decay of unedited transcript with a premature stop codon in exon 45. These findings indicate that the scAAV system is highly efficient in inducing INDELs at the targeted genomic locus, and most of the INDEL events contain +1-nt insertions, which is able to repair the out-of-frame mutation in *Dmd* exon 45.

Next, we performed quantitative polymerase chain reaction (PCR) analysis to detect viral genome copies in the skeletal muscles and heart

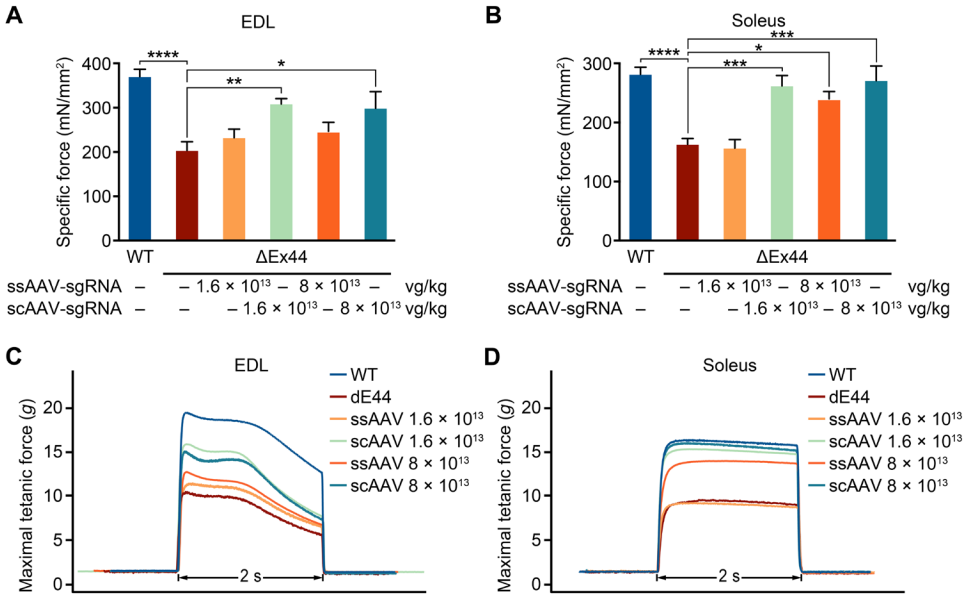


**Fig. 4. Rescue of skeletal muscle function after systemic AAV delivery of CRISPR-Cas9 genome editing components.** (**A** and **B**) Specific force (mN/mm$^2$) of the extensor digitorum longus (EDL) (A) and soleus (B) muscles in WT, ΔEx44 mice untreated, and ΔEx44 mice treated with ssAAV-packaged *Sp*Cas9 and scAAV- or ssAAV-packaged sgRNA. The *Sp*Cas9 vector was kept at a constant dose of $8 \times 10^{13}$ vg/kg. The dose of the sgRNA vector is shown in the figure. Data are presented as mean ± SEM. One-way ANOVA was performed with post hoc Tukey's multiple comparisons test. *$P < 0.05$, **$P < 0.005$, ***$P < 0.001$, ****$P < 0.0001$ ($n = 6$). (**C** and **D**) Maximal tetanic force of the EDL (C) and soleus (D) muscles in WT, ΔEx44 untreated mice, and ΔEx44 mice treated with ssAAV-packaged *Sp*Cas9 and scAAV- or ssAAV-packaged sgRNA. The *Sp*Cas9 vector was kept at a constant dose of $8 \times 10^{13}$ vg/kg. The dose of the sgRNA vector is shown in the figure ($n = 6$).

of ΔEx44 mice 4 weeks after systemic delivery of AAV–CRISPR-Cas9 genome editing components. Mice receiving scAAV treatment showed significantly higher copy numbers of sgRNA viral genomes than those receiving the same dose of ssAAV-packaged sgRNA (Fig. 6A). Moreover, the sgRNA transcripts transcribed from the scAAV vector were also significantly higher than those transcribed from the ssAAV vector (fig. S8A). These findings indicate that there is a substantial depletion of the ssAAV-packaged sgRNA vector in skeletal muscles in vivo. Although the dose of the Cas9 vector was kept constant at $8 \times 10^{13}$ vg/kg during initial systemic injection, the viral genomes of the Cas9 vector in the TA and triceps persisted with higher copies from mice receiving the scAAV-packaged sgRNA vector than those receiving the same dose of the ssAAV-packaged sgRNA vector (Fig. 6B). However, AAV-Cas9 viral genomes showed relatively high copies in the diaphragm and heart independent of the identity of AAV-sgRNA vector (Fig. 6B). These findings are consistent with Cas9 cDNA transcript analysis (fig. S8B). Together, these data suggest that the high efficiency of scAAV-mediated in vivo genome editing is attributed to higher viral genome persistence of the sgRNA vector and Cas9 vector.

## DISCUSSION

Owing to nonpathogenic and low-immunogenic characteristics, recombinant AAV has been chosen as a delivery vector for multiple gene therapy clinical trials, and three have been approved for treating lipoprotein lipase deficiency, inherited retinal dystrophy, and spinal muscular atrophy (*39*). In this study, we developed a new genome editing strategy in which the Cas9 nuclease is encoded by conventional ssAAV, while sgRNAs are expressed by double-stranded scAAV. After a single high-dose systemic injection of this dual AAV system into ΔEx44 mice (Cas9 vector, $8 \times 10^{13}$ vg/kg; sgRNA vector, $8 \times 10^{13}$ vg/kg), dystrophin protein expression in multiple muscle groups was restored by ~80%, and skeletal muscle function was improved by ~82% in fast-twitch EDL muscle and by ~96% in slow-twitch soleus muscle. A low dose of scAAV-expressed sgRNAs ($4 \times 10^{12}$ vg/kg) is sufficient to restore 18, 14, and 50% of dystrophin protein in the TA, triceps, and diaphragm, respectively, representing a 20-fold improvement in efficiency compared with the ssAAV-packaged sgRNA vector. Several potential explanations may account for these observations. First, it has been widely accepted that most recombinant AAV genomes persist as double-stranded episomes in vivo, in the form of either circular or linear concatemers (*40*–*42*). During the concatemerization process, the double-stranded DNA intermediate is an indispensable prerequisite. Thus, the scAAV undergoes concatemerization more rapidly than ssAAV because scAAV-based concatemerization bypasses second-strand synthesis, which is a rate-limiting step for ssAAV (*31*, *32*). Second, it has been reported that monomeric viral genome degradation is slower in scAAV-transduced skeletal muscle compared with ssAAV (*33*). Therefore, scAAV is more stable than ssAAV during initial viral transduction, leading to higher episomal persistence in the long term. Third, DNA DSBs in postmitotic cells are repaired by the classical NHEJ pathway, which requires the catalytic subunit of DNA-dependent protein kinase (DNA-PKcs) (*43*). It is known that DNA-PKcs is required for AAV viral genome concatemerization in AAV-transduced skeletal muscle (*44*). In this study, we found that scAAV-packaged sgRNA leads to a higher incidence of DNA DSB at the target site. This may induce higher DNA-PKcs expression, which, in turn, facilitates AAV concatemerization and long-term gene expression. We found higher viral genome persistence of both sgRNA vector and Cas9 vector in mice treated with scAAV-packaged sgRNA. In summary, the scAAV-sgRNA delivery system has many appealing features, including stable persistence of AAV viral genomes, higher INDEL frequency at the

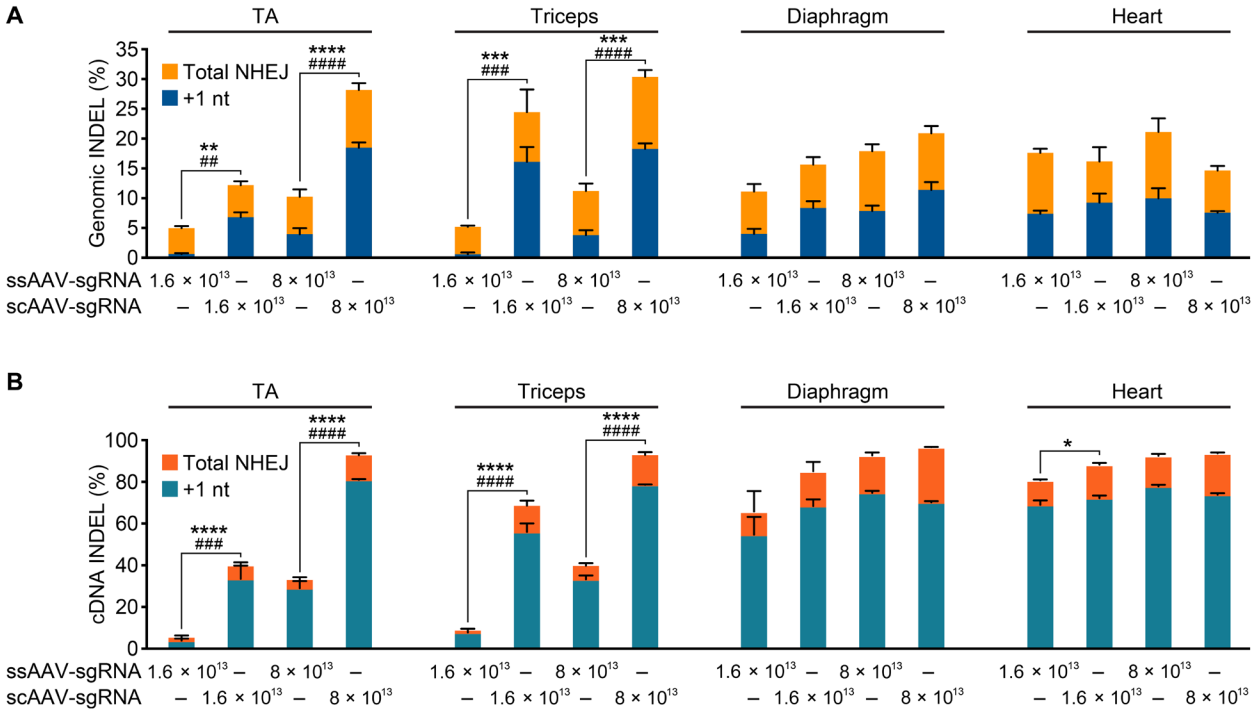


**Fig. 5. The scAAV vector induces significant INDELs at the genomic and cDNA level.** (**A** and **B**) Genomic INDEL analysis by deep sequencing (A) and dystrophin cDNA INDEL analysis by TIDE analysis (B) of the TA, triceps, diaphragm, and heart of ΔEx44 mice 4 weeks after systemic delivery of ssAAV-packaged *Sp*Cas9 and scAAV or ssAAV-packaged sgRNA. The *Sp*Cas9 vector was kept at a constant dose of $8 \times 10^{13}$ vg/kg. The dose of the sgRNA vector is shown in the figure. Data are presented as mean ± SEM. Two-way ANOVA was performed with post hoc Tukey's multiple comparisons test. **P* < 0.05, ***P* < 0.005, ****P* < 0.001, *****P* < 0.0001 for the total NHEJ event (*n* = 3). ##*P* < 0.005, ###*P* < 0.001, ####*P* < 0.0001 for the +1-nt insertion event (*n* = 3).

targeted genomic locus, and highly efficient genome editing in vitro and in vivo at low viral dose.

Initial studies of Cas9-induced DNA DSBs suggested that the breakage point was blunt-ended (*12*, *45*). However, molecular dynamics simulations of the *Sp*Cas9-sgRNA-dsDNA system suggest that *Sp*Cas9-induced cleavage generates a staggered cut, producing a single nucleotide 5′ overhang at the breakage point, which is prone to be filled with one additional nucleotide by the DNA polymerase, leading to a high frequency of +1-nt insertion after NHEJ-mediated repair (*46*, *47*). On the basis of this mechanism, our laboratory developed CRISPR-Cas9–mediated "single-cut" technology and successfully restored the ORF of *Dmd* exon 51 in mice and dogs with exon 50 deletion and *Dmd* exon 45 ORF in mice lacking exon 44 (*23*–*25*). This technology, in theory, can be applied to correct diverse mutations in any exon containing a single-nucleotide out-of-frame deletion (*48*). However, there remains another group of mutations in which the frameshift mutation needs to be reframed by 3n + 2 insertions or 3n − 1 deletion. In such cases, the CRISPR-Cas9–mediated "single-cut" repair strategy may be less efficient. Several studies have shown that it is possible to restore the *Dmd* ORF by removing one or multiple exons by using two sgRNAs (*17*–*22*). However, this "double-cut" strategy is only effective when two cooperative DNA DSBs occur simultaneously. If the first DNA DSB is rapidly rejoined by NHEJ-mediated repair, then the second DSB alone is not sufficient to excise the entire exon. Moreover, a high frequency of AAV ITR integration events is observed at the Cas9 target site when two sgRNAs are used to excise large genomic intervening regions (*22*, *49*). Therefore, the CRISPR-Cas9–mediated "single-cut" repair strategy has unique advantages, including predictable DNA repair outcome, minimum genomic modification at a precise location, and low frequency of off-target effects.

Nevertheless, many questions remain unaddressed for AAV-delivered CRISPR-Cas9–mediated therapeutic genome editing. The first concern is the potential for adaptive immune responses elicited by AAV capsid protein and Cas9 nuclease. It has been reported that AAV-neutralizing antibodies, anti-*Sp*Cas9 antibodies, and *Sp*Cas9-specific T cells are found in the human population (*50*–*53*). While no apparent immune response to AAV or Cas9 was observed in neonatal mice, it remains unclear whether this observation will also apply to humans. Potential solutions to address these concerns include (i) large-scale functional variant profiling of AAV and *Sp*Cas9 for epitope mutagenesis to block antibody binding, (ii) plasmapheresis to reduce neutralizing antibody titer, and (iii) transient immunosuppression (*54*). The second concern is durability of CRISPR-Cas9–mediated therapeutic genome editing. Our deep sequencing analysis in multiple skeletal muscle samples showed an average of 21% editing events at the genomic level, among which, 75% of editing events are effective and able to restore the *Dmd* ORF. Moreover, recent studies in the *mdx* mouse model of DMD showed that sustained genome editing and dystrophin expression can be observed for 12 to 18 months after a single intravenous injection of AAV9-encoded *Sa*Cas9 (Cas9 derived from *Staphylococcus aureus*) (*21*, *22*). However, skeletal muscle contains stem cells capable of undergoing de novo myogenesis and contributing to preexisting myofibers (*55*). Whether these events will gradually dilute out genome-edited, dystrophin-positive myofibers in the long term remains to be determined. In this study, we were able to restore more than 70% of dystrophin expression in the heart. In addition, adult human cardiomyocytes

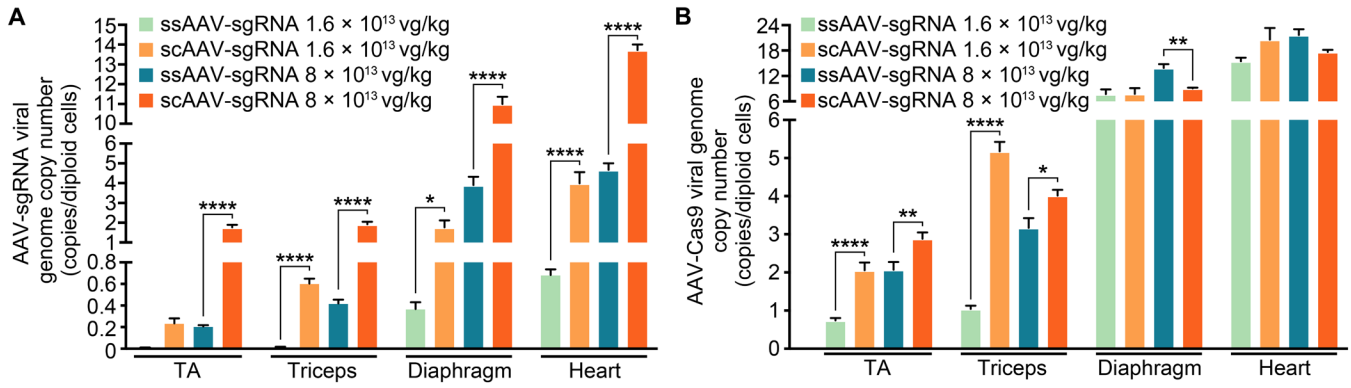


**Fig. 6. ΔEx44 mice sustain higher copies of viral genome after systemic delivery of scAAV-packaged sgRNA.** (**A** and **B**) sgRNA viral genome copy number (A) and Cas9 viral genome copy number (B) quantification from skeletal muscles and heart of ΔEx44 mice 4 weeks after systemic delivery of ssAAV-packaged *Sp*Cas9 and scAAV- or ssAAV-packaged sgRNA. The *Sp*Cas9 vector was kept at a constant dose of $8 \times 10^{13}$ vg/kg. The dose of the sgRNA vector is shown in the figure. Data are presented as mean ± SEM. One-way ANOVA was performed with post hoc Tukey's multiple comparisons test. $^{*}P < 0.05$, $^{**}P < 0.005$, $^{****}P < 0.0001$ ($n = 3$).

have a very low turnover rate (from 1% at the age of 25 to 0.45% at the age of 75) (*56*, *57*). Thus, in theory, long-term clinical benefit by CRISPR-Cas9–mediated genome editing should be sustained in the human heart.

In summary, a low dose of scAAV-delivered CRISPR-Cas genome editing components is sufficient to restore dystrophin protein expression, reduce DMD pathological phenotypes, and improve muscle function in a DMD mouse model. Therefore, this robust scAAV delivery system combined with the efficient CRISPR-Cas9 genome editing technology represents a promising therapy for permanent correction of diverse genetic mutations in neuromuscular diseases.

## MATERIALS AND METHODS

### Study design

This study was designed with the primary aim of investigating the feasibility of using the scAAV system to deliver the CRISPR-Cas9 genome editing components for the correction of DMD mutations. The secondary objective was to compare the efficiency between the conventional ssAAV and scAAV in delivering CRISPR sgRNA for in vivo therapeutic genome editing. We did not use exclusion, randomization, or blind approaches to assign the animals for the experiments. For each experiment, sample size reflects the number of independent biological replicates and was provided in the figure legends.

### AAV vector cloning and viral production

The sgRNA targeting mouse *Dmd* exon 45, listed in table S2, was first cloned into TRISPR-sgRNA-CK8e–green fluorescent protein plasmid, a modified gift from D. Grimm, using Golden Gate Assembly (New England Biolabs). A detailed cloning protocol was previously described (*23*). The sgRNA expression cassette containing three copies of the same sgRNA driven by the U6, H1, and 7SK promoter was PCR-amplified and subcloned into the pSJG scAAV plasmid, a gift from S. Gray, or into the pSSV9 single-stranded AAV plasmid (ssAAV plasmid), using In-Fusion Cloning Kit (Takara Bio). A 2.3-kb stuffer sequence was cloned into the ssAAV plasmid for optimal viral packaging. Both the scAAV and the ssAAV genome contain the same sgRNA expression cassette, consisting of three copies of sgRNA sequence driven by three RNA polymerase III promoters. Cloning primers are listed in table S2. All AAV viral plasmids were column-purified and digested with Sma I and Ahd I to check ITR integrity. AAVs were packaged by Boston Children's Hospital Viral Core, and serotype 9 was chosen for capsid assembly. AAV titers were determined by Droplet Digital PCR (Bio-Rad Laboratories) according to the manufacturer's protocol. Primers and probes used for titration are listed in table S2.

### Alkaline agarose gel electrophoresis

AAV virus ($2 \times 10^{11}$ vg) was equalized with water to 13 μl and digested with 10 μl of deoxyribonuclease (DNase) solution [10 mM tris-HCl (pH 7.5), 10 mM $CaCl_2$, 10 mM $MgCl_2$, and DNase (0.1 mg/ml)] at 37°C for 1 hour, followed by chelating $Mg^{2+}$ and $Ca^{2+}$ with 5 μl of 0.5 M EDTA. Then, the capsid was denatured by adding 2 μl of 10% SDS. The reaction mixture was mixed with 6 μl of 6× alkaline agarose gel loading dye (Alfa Aesar) and loaded into 1% alkaline agarose gel. Denaturing gel electrophoresis was performed in a cold room at 50 V for 15 hours. The gel was neutralized with neutralization buffer [0.5 M tris-HCl (pH 7.5) and 1 M NaCl] and stained with SYBR Gold (Thermo Fisher Scientific) for visualization.

### In vitro AAV viral transduction in C2C12 myotubes

Cas9-expressing C2C12 myoblasts were cultured in 96-well dishes with growth medium [Dulbecco's modified Eagle's medium (DMEM) with 10% fetal bovine serum] until reaching 90% confluency. Then, the myoblasts were allowed to differentiate in myotubes in differentiation medium (DMEM with 2% horse serum) for 5 days. Two hours before viral transduction, myotubes were treated with *Vibrio cholerae* neuraminidase (50 mU/ml) (Sigma-Aldrich), followed by washing with differentiation medium twice (*58*). Myotubes were incubated with varying doses of scAAV or ssAAV and centrifuged at 1000*g* at 4°C for 1.5 hours. After spin transduction, the virus was aspirated, and the myotubes were washed with differentiation medium three times. The myotubes were cultured in differentiation medium for an additional week before genomic DNA isolation for INDEL analysis.

### In vivo AAV delivery into ΔEx44 mice

Postnatal day 4 ΔEx44 mice were injected intraperitoneally with 80 μl of AAV9 viral mixture containing AAV9-*Sp*Cas9 ($8 \times 10^{13}$ vg/kg)

and varying doses of scAAV- or ssAAV-packaged sgRNA using an ultrafine BD insulin syringe (Becton Dickinson). The doses of scAAV- or ssAAV-packaged sgRNA are indicated in the figure legends. Four weeks after systemic delivery, ΔEx44 mice and WT littermates were dissected for physiological, biochemical, and histological analysis. Animal work described in this manuscript has been approved and conducted under the oversight of the University of Texas Southwestern Institutional Animal Care and Use Committee.

### Genomic DNA and RNA isolation, cDNA synthesis, and PCR amplification

Genomic DNA of mouse C2C12 myotubes, skeletal muscles, and heart was isolated using DirectPCR (cell) Lysis Reagent (Viagen Biotech) according to the manufacturer's protocol. Total RNA of skeletal muscles and heart was isolated using miRNeasy (QIAGEN) according to the manufacturer's protocol. cDNA was reverse-transcribed from total RNA using SuperScript III First-Strand Synthesis SuperMix (Thermo Fisher Scientific) according to the manufacturer's protocol. PCR amplification was performed as previously described (*25*). Primer sequences are listed in table S2.

### INDEL analysis of cDNA

INDELs in cDNA were analyzed using the TIDE software package (https://tide.deskgen.com). Briefly, the sgRNA sequence targeting mouse *Dmd* exon 45 was first uploaded to the software to define *Sp*Cas9-mediated DSB site. Then, the CRISPR-Cas9–edited sequence and non-edited control sequence were uploaded and aligned using Smith-Waterman local alignment algorithm. The percentage of INDELs was calculated on the basis of the relative abundance of aberrant nucleotides over the length of the whole sequence trace.

### Amplicon deep sequencing analysis of genomic DNA

PCR of genomic DNA was performed using primers designed against the *Dmd* exon 45 region. A second round of PCR was performed to add Illumina flow cell binding sequence and barcodes. All primer sequences are listed in table S2. Deep sequencing and data analysis were performed as previously described (*25*).

### AAV viral genome copy number quantification

The AAV viral genome copy number was determined by quantitative PCR using custom-designed primers (table S2). The primer sets used in AAV-sgRNA and AAV-Cas9 viral genome quantification were annealed to the 7SK promoter and Cas9 gene, respectively. The threshold cycle value of each reaction was converted to the viral genome copy number by measuring against the copy number standard curve of the AAV plasmids used for AAV packaging in this study. Mouse 18*S* ribosomal RNA gene was used as the reference gene to calibrate genomic DNA quantity.

### Dystrophin and *Sp*Cas9 Western blot analysis

Heart and skeletal muscles were crushed and lysed with lysis buffer [10% SDS, 62.5 mM tris (pH 6.8), 1 mM EDTA, and protease inhibitor]. A total of 50 μg of protein was loaded onto 4 to 20% Criterion TGX Precast Midi Protein Gel (Bio-Rad Laboratories). Details of Western blot running, transferring, and developing were previously described (*25*). Primary antibodies used in Western blot were mouse anti-dystrophin antibody (MANDYS8, Sigma-Aldrich, D8168), mouse anti-Cas9 antibody (Clone 7A9, Millipore, MAC133), and mouse anti-vinculin antibody (Sigma-Aldrich, V9131). Secondary antibodies used in Western blot were goat anti-mouse horseradish peroxidase (HRP) antibody or goat anti-rabbit HRP antibody (Bio-Rad Laboratories).

### Histological analysis of skeletal muscle and heart

Skeletal muscles and heart were cryosectioned into 8-μm transverse sections. Immunohistochemistry was performed as previously described (*25*). Antibodies used in immunohistochemistry were mouse anti-dystrophin antibody (MANDYS8, Sigma-Aldrich, D8168) and Mouse on Mouse biotinylated anti-mouse IgG (BMK-2202, Vector Laboratories).

### Electrophysiological analysis of isolated EDL and soleus muscles

Four weeks after systemic AAV–CRISPR-Cas9 genome editing, EDL and soleus muscles from ΔEx44 mice and WT littermates were isolated for electrophysiological analysis, as previously described (*25*). Specific force ($mN/mm^2$) was calculated by normalizing contraction force to muscle cross-sectional area.

### Statistics

All data are shown as means ± SEM. One-way analysis of variance (ANOVA) or two-way ANOVA was performed with post hoc Tukey's multiple comparisons test. $P < 0.05$ was considered statistically significant.

## SUPPLEMENTARY MATERIALS

Supplementary material for this article is available at http://advances.sciencemag.org/cgi/content/full/6/8/eaay6812/DC1

Fig. S1. Alkaline denaturing gel electrophoresis confirms integrity of AAV vectors.
Fig. S2. Systemic delivery of CRISPR-Cas9 genome editing components by single-stranded AAV vector to ΔEx44 mice rescues dystrophin expression.
Fig. S3. Whole muscle scanning of immunohistochemistry of TA, triceps, diaphragm, and heart of CRISPR-Cas9–corrected ΔEx44 mice.
Fig. S4. Western blot analysis of skeletal muscles and heart of ΔEx44 mice treated with ssAAV-packaged CRISPR-Cas9 genome editing components.
Fig. S5. Muscle histology of ΔEx44 mice after systemic delivery of AAV expressing CRISPR-Cas9 genome editing components.
Fig. S6. Whole-muscle scanning of H&E staining of TA, triceps, diaphragm, and heart of CRISPR-Cas9–corrected ΔEx44 mice.
Fig. S7. Serum CK analysis of CRISPR-Cas9–corrected ΔEx44 mice.
Fig. S8. ΔEx44 mice express more Cas9 and sgRNA transcripts after systemic delivery of scAAV-packaged sgRNA.
Table S1. Deep sequencing analysis of CRISPR-Cas9–corrected ΔEx44 mice.
Table S2. Primers used in this study.

## REFERENCES AND NOTES

1. E. P. Hoffman, R. H. Brown Jr., L. M. Kunkel, Dystrophin: The protein product of the Duchenne muscular dystrophy locus. *Cell* **51**, 919–928 (1987).
2. M. Koenig, E. P. Hoffman, C. J. Bertelson, A. P. Monaco, C. Feener, L. M. Kunkel, Complete cloning of the Duchenne muscular dystrophy (DMD) cDNA and preliminary genomic organization of the DMD gene in normal and affected individuals. *Cell* **50**, 509–517 (1987).
3. Q. Gao, E. M. McNally, The dystrophin complex: Structure, function, and implications for therapy. *Compr. Physiol.* **5**, 1223–1239 (2015).
4. S. Guiraud, A. Aartsma-Rus, N. M. Vieira, K. E. Davies, G.-J. B. van Ommen, L. M. Kunkel, The pathogenesis and therapy of muscular dystrophies. *Annu. Rev. Genomics Hum. Genet.* **16**, 281–308 (2015).
5. K. P. Campbell, S. D. Kahl, Association of dystrophin and an integral membrane glycoprotein. *Nature* **338**, 259–262 (1989).
6. A. Aartsma-Rus, J. C. T. Van Deutekom, I. F. Fokkema, G.-J. Van Ommen, J. T. Den Dunnen, Entries in the Leiden Duchenne muscular dystrophy mutation database: An overview of mutation types and paradoxical cases that confirm the reading-frame rule. *Muscle Nerve* **34**, 135–144 (2006).

7. C. L. Bladen, D. Salgado, S. Monges, M. E. Foncuberta, K. Kekou, K. Kosma, H. Dawkins, L. Lamont, A. J. Roy, T. Chamova, V. Guergueltcheva, S. Chan, L. Korngut, C. Campbell, Y. Dai, J. Wang, N. Barišić, P. Brabec, J. Lahdetie, M. C. Walter, O. Schreiber-Katz, V. Karcagi, M. Garami, V. Viswanathan, F. Bayat, F. Buccella, E. Kimura, Z. Koeks, J. C. van den Bergen, M. Rodrigues, R. Roxburgh, A. Lusakowska, A. Kostera-Pruszczyk, J. Zimowski, R. Santos, E. Neagu, S. Artemieva, V. M. Rasic, D. Vojinovic, M. Posada, C. Bloetzer, P.-Y. Jeannet, F. Joncourt, J. Díaz-Manera, E. Gallardo, A. A. Karaduman, H. Topaloğlu, R. El Sherif, A. Stringer, A. V. Shatillo, A. S. Martin, H. L. Peay, M. I. Bellgard, J. Kirschner, K. M. Flanigan, V. Straub, K. Bushby, J. Verschuuren, A. Aartsma-Rus, C. Béroud, H. Lochmüller, The TREAT-NMD DMD Global Database: Analysis of more than 7,000 Duchenne muscular dystrophy mutations. *Hum. Mutat.* **36**, 395–402 (2015).
8. K. Bushby, F. Muntoni, A. Urtizberea, R. Hughes, R. Griggs, Report on the 124th ENMC International Workshop. Treatment of Duchenne muscular dystrophy; defining the gold standards of management in the use of corticosteroids. 2-4 April 2004, Naarden, The Netherlands. *Neuromuscul. Disord.* **14**, 526–534 (2004).
9. J. S. Charleston, F. J. Schnell, J. Dworzak, C. Donoghue, S. Lewis, L. Chen, G. D. Young, A. J. Milici, J. Voss, U. DeAlwis, B. Wentworth, L. R. Rodino-Klapac, Z. Sahenk, D. Frank, J. R. Mendell, Eteplirsen treatment for Duchenne muscular dystrophy. *Neurology* **90**, e2146–e2154 (2018).
10. D. Duan, Systemic AAV micro-dystrophin gene therapy for Duchenne muscular dystrophy. *Mol. Ther.* **26**, 2337–2356 (2018).
11. L. Cong, F. A. Ran, D. Cox, S. Lin, R. Barretto, N. Habib, P. D. Hsu, X. Wu, W. Jiang, L. A. Marraffini, F. Zhang, Multiplex genome engineering using CRISPR/Cas systems. *Science* **339**, 819–823 (2013).
12. M. Jinek, K. Chylinski, I. Fonfara, M. Hauer, J. A. Doudna, E. Charpentier, A programmable dual-RNA–guided DNA endonuclease in adaptive bacterial immunity. *Science* **337**, 816–821 (2012).
13. P. Mali, L. Yang, K. M. Esvelt, J. Aach, M. Guell, J. E. DiCarlo, J. E. Norville, G. M. Church, RNA-guided human genome engineering via Cas9. *Science* **339**, 823–826 (2013).
14. C. Long, J. R. McAnally, J. M. Shelton, A. A. Mireault, R. Bassel-Duby, E. N. Olson, Prevention of muscular dystrophy in mice by CRISPR/Cas9-mediated editing of germline DNA. *Science* **345**, 1184–1188 (2014).
15. Y. Zhang, C. Long, H. Li, J. R. McAnally, K. K. Baskin, J. M. Shelton, R. Bassel-Duby, E. N. Olson, CRISPR-Cpf1 correction of muscular dystrophy mutations in human cardiomyocytes and mice. *Sci. Adv.* **3**, e1602814 (2017).
16. P. Zhu, F. Wu, J. Mosenson, H. Zhang, T.-C. He, W.-S. Wu, CRISPR/Cas9-mediated genome editing corrects dystrophin mutation in skeletal muscle stem cells in a mouse model of muscle dystrophy. *Mol. Ther. Nucleic Acids* **7**, 31–41 (2017).
17. C. Long, L. Amoasii, A. A. Mireault, J. R. McAnally, H. Li, E. Sanchez-Ortiz, S. Bhattacharyya, J. M. Shelton, R. Bassel-Duby, E. N. Olson, Postnatal genome editing partially restores dystrophin expression in a mouse model of muscular dystrophy. *Science* **351**, 400–403 (2016).
18. C. E. Nelson, C. H. Hakim, D. G. Ousterout, P. I. Thakore, E. A. Moreb, R. M. C. Rivera, S. Madhavan, X. Pan, F. A. Ran, W. X. Yan, A. Asokan, F. Zhang, D. Duan, C. A. Gersbach, In vivo genome editing improves muscle function in a mouse model of Duchenne muscular dystrophy. *Science* **351**, 403–407 (2016).
19. M. Tabebordbar, K. Zhu, J. K. W. Cheng, W. L. Chew, J. J. Widrick, W. X. Yan, C. Maesner, E. Y. Wu, R. Xiao, F. A. Ran, L. Cong, F. Zhang, L. H. Vandenberghe, G. M. Church, A. J. Wagers, In vivo gene editing in dystrophic mouse muscle and muscle stem cells. *Science* **351**, 407–411 (2016).
20. N. E. Bengtsson, J. K. Hall, G. L. Odom, M. P. Phelps, C. R. Andrus, R. D. Hawkins, S. D. Hauschka, J. R. Chamberlain, J. S. Chamberlain, Muscle-specific CRISPR/Cas9 dystrophin gene editing ameliorates pathophysiology in a mouse model for Duchenne muscular dystrophy. *Nat. Commun.* **8**, 14454 (2017).
21. C. H. Hakim, N. B. Wasala, C. E. Nelson, L. P. Wasala, Y. Yue, J. A. Louderman, T. B. Lessa, A. Dai, K. Zhang, G. J. Jenkins, M. E. Nance, X. Pan, K. Kodippili, N. N. Yang, S.-j. Chen, C. A. Gersbach, D. Duan, AAV CRISPR editing rescues cardiac and muscle function for 18 months in dystrophic mice. *JCI Insight* **3**, e124297 (2018).
22. C. E. Nelson, Y. Wu, M. P. Gemberling, M. L. Oliver, M. A. Waller, J. D. Bohning, J. N. Robinson-Hamm, K. Bulaklak, R. M. Castellanos Rivera, J. H. Collier, A. Asokan, C. A. Gersbach, Long-term evaluation of AAV-CRISPR genome editing for Duchenne muscular dystrophy. *Nat. Med.* **25**, 427–432 (2019).
23. L. Amoasii, C. Long, H. Li, A. A. Mireault, J. M. Shelton, E. Sanchez-Ortiz, J. R. McAnally, S. Bhattacharyya, F. Schmidt, D. Grimm, S. D. Hauschka, R. Bassel-Duby, E. N. Olson, Single-cut genome editing restores dystrophin expression in a new mouse model of muscular dystrophy. *Sci. Transl. Med.* **9**, eaan8081 (2017).
24. L. Amoasii, J. C. W. Hildyard, H. Li, E. Sanchez-Ortiz, A. Mireault, D. Caballero, R. Harron, T.-R. Stathopoulou, C. Massey, J. M. Shelton, R. Bassel-Duby, R. J. Piercy, E. N. Olson, Gene editing restores dystrophin expression in a canine model of Duchenne muscular dystrophy. *Science* **362**, 86–91 (2018).
25. Y.-L. Min, H. Li, C. Rodriguez-Caycedo, A. A. Mireault, J. Huang, J. M. Shelton, J. R. McAnally, L. Amoasii, P. P. A. Mammen, R. Bassel-Duby, E. N. Olson, CRISPR-Cas9 corrects Duchenne muscular dystrophy exon 44 deletion mutations in mice and human cells. *Sci. Adv.* **5**, eaav4324 (2019).
26. R. J. Samulski, N. Muzyczka, AAV-mediated gene therapy for research and therapeutic purposes. *Annu. Rev. Virol.* **1**, 427–451 (2014).
27. J. N. Kornegay, J. Li, J. R. Bogan, D. J. Bogan, C. Chen, H. Zheng, B. Wang, C. Qiao, J. F. Howard Jr., X. Xiao, Widespread muscle expression of an AAV9 human mini-dystrophin vector after intravenous injection in neonatal dystrophin-deficient dogs. *Mol. Ther.* **18**, 1501–1508 (2010).
28. C. Hinderer, N. Katz, E. L. Buza, C. Dyer, T. Goode, P. Bell, L. K. Richman, J. M. Wilson, Severe toxicity in nonhuman primates and piglets following high-dose intravenous administration of an adeno-associated virus vector expressing human SMN. *Hum. Gene Ther.* **29**, 285–298 (2018).
29. D. M. McCarty, H. Fu, P. E. Monahan, C. E. Toulson, P. Naik, R. J. Samulski, Adeno-associated virus terminal repeat (TR) mutant generates self-complementary vectors to overcome the rate-limiting step to transduction in vivo. *Gene Ther.* **10**, 2112–2118 (2003).
30. Z. Wang, H.-I. Ma, J. Li, L. Sun, J. Zhang, X. Xiao, Rapid and highly efficient transduction by double-stranded adeno-associated virus vectors in vitro and in vivo. *Gene Ther.* **10**, 2105–2111 (2003).
31. F. K. Ferrari, T. Samulski, T. Shenk, R. J. Samulski, Second-strand synthesis is a rate-limiting step for efficient transduction by recombinant adeno-associated virus vectors. *J. Virol.* **70**, 3227–3234 (1996).
32. K. J. Fisher, G. P. Gao, M. D. Weitzman, R. DeMatteo, J. F. Burda, J. M. Wilson, Transduction with recombinant adeno-associated virus for gene therapy is limited by leading-strand synthesis. *J. Virol.* **70**, 520–532 (1996).
33. C. Ren, S. Kumar, D. R. Shaw, S. Ponnazhagan, Genomic stability of self-complementary adeno-associated virus 2 during early stages of transduction in mouse muscle in vivo. *Hum. Gene Ther.* **16**, 1047–1057 (2005).
34. D. M. McCarty, Self-complementary AAV vectors; advances and applications. *Mol. Ther.* **16**, 1648–1656 (2008).
35. J. R. Mendell, S. Al-Zaidy, R. Shell, W. D. Arnold, L. R. Rodino-Klapac, T. W. Prior, L. Lowes, L. Alfano, K. Berry, K. Church, J. T. Kissel, S. Nagendran, J. L'Italien, D. M. Sproule, C. Wells, J. A. Cardenas, M. D. Heitzer, A. Kaspar, S. Corcoran, L. Braun, S. Likhite, C. Miranda, K. Meyer, K. D. Foust, A. H. M. Burghes, B. K. Kaspar, Single-dose gene-replacement therapy for spinal muscular atrophy. *N. Engl. J. Med.* **377**, 1713–1722 (2017).
36. E. R. Pozsgai, D. A. Griffin, K. N. Heller, J. R. Mendell, L. R. Rodino-Klapac, Systemic AAV-mediated β-sarcoglycan delivery targeting cardiac and skeletal muscle ameliorates histological and functional deficits in LGMD2E mice. *Mol. Ther.* **25**, 855–869 (2017).
37. K. Inagaki, S. Fuess, T. A. Storm, G. A. Gibson, C. F. Mctiernan, M. A. Kay, H. Nakai, Robust systemic transduction with AAV9 vectors in mice: Efficient global cardiac gene transfer superior to that of AAV8. *Mol. Ther.* **14**, 45–53 (2006).
38. C. L. Himeda, X. Chen, S. D. Hauschka, Design and testing of regulatory cassettes for optimal activity in skeletal and cardiac muscles. *Methods Mol. Biol.* **709**, 3–19 (2011).
39. C. E. Dunbar, K. A. High, J. K. Joung, D. B. Kohn, K. Ozawa, M. Sadelain, Gene therapy comes of age. *Science* **359**, eaan4672 (2018).
40. D. Duan, P. Sharma, J. Yang, Y. Yue, L. Dudus, Y. Zhang, K. J. Fisher, J. F. Engelhardt, Circular intermediates of recombinant adeno-associated virus have defined structural characteristics responsible for long-term episomal persistence in muscle tissue. *J. Virol.* **72**, 8568–8577 (1998).
41. C. H. Miao, R. O. Snyder, D. B. Schowalter, G. A. Patijn, B. Donahue, B. Winther, M. A. Kay, The kinetics of rAAV integration in the liver. *Nat. Genet.* **19**, 13–15 (1998).
42. H. Nakai, S. R. Yant, T. A. Storm, S. Fuess, L. Meuse, M. A. Kay, Extrachromosomal recombinant adeno-associated virus vector genomes are primarily responsible for stable liver transduction in vivo. *J. Virol.* **75**, 6969–6976 (2001).
43. A. Ciccia, S. J. Elledge, The DNA damage response: Making it safe to play with knives. *Mol. Cell* **40**, 179–204 (2010).
44. D. Duan, Y. Yue, J. F. Engelhardt, Consequences of DNA-dependent protein kinase catalytic subunit deficiency on recombinant adeno-associated virus genome circularization and heterodimerization in muscle tissue. *J. Virol.* **77**, 4751–4759 (2003).
45. G. Gasiunas, R. Barrangou, P. Horvath, V. Siksnys, Cas9-crRNA ribonucleoprotein complex mediates specific DNA cleavage for adaptive immunity in bacteria. *Proc. Natl. Acad. Sci. U.S.A.* **109**, E2579–E2586 (2012).
46. Z. Zuo, J. Liu, Cas9-catalyzed DNA cleavage generates staggered ends: Evidence from molecular dynamics simulations. *Sci. Rep.* **5**, 37584 (2016).
47. B. R. Lemos, A. C. Kaplan, J. E. Bae, A. E. Ferrazzoli, J. Kuo, R. P. Anand, D. P. Waterman, J. E. Haber, CRISPR/Cas9 cleavages in budding yeast reveal templated insertions and strand-specific insertion/deletion profiles. *Proc. Natl. Acad. Sci. U.S.A.* **115**, E2040–E2047 (2018).
48. C. Long, H. Li, M. Tiburcy, C. Rodriguez-Caycedo, V. Kyrychenko, H. Zhou, Y. Zhang, Y.-L. Min, J. M. Shelton, P. P. A. Mammen, N. Y. Liaw, W.-H. Zimmermann, R. Bassel-Duby, J. W. Schneider, E. N. Olson, Correction of diverse muscular dystrophy mutations in human engineered heart muscle by single-site genome editing. *Sci. Adv.* **4**, eaap9004 (2018).

49. M. L. Maeder, M. Stefanidakis, C. J. Wilson, R. Baral, L. A. Barrera, G. S. Bounoutas, D. Bumcrot, H. Chao, D. M. Ciulla, J. A. DaSilva, A. Dass, V. Dhanapal, T. J. Fennell, A. E. Friedland, G. Giannoukos, S. W. Gloskowski, A. Glucksmann, G. M. Gotta, H. Jayaram, S. J. Haskett, B. Hopkins, J. E. Horng, S. Joshi, E. Marco, R. Mepani, D. Reyon, T. Ta, D. G. Tabbaa, S. J. Samuelsson, S. Shen, M. N. Skor, P. Stetkiewicz, T. Wang, C. Yudkoff, V. E. Myer, C. F. Albright, H. Jiang, Development of a gene-editing approach to restore vision loss in Leber congenital amaurosis type 10. *Nat. Med.* **25**, 229–233 (2019).
50. R. Calcedo, L. H. Vandenberghe, G. Gao, J. Lin, J. M. Wilson, Worldwide epidemiology of neutralizing antibodies to adeno-associated viruses. *J. Infect. Dis.* **199**, 381–390 (2009).
51. S. Boutin, V. Monteilhet, P. Veron, C. Leborgne, O. Benveniste, M. F. Montus, C. Masurier, Prevalence of serum IgG and neutralizing factors against adeno-associated virus (AAV) types 1, 2, 5, 6, 8, and 9 in the healthy population: Implications for gene therapy using AAV vectors. *Hum. Gene Ther.* **21**, 704–712 (2010).
52. W. L. Chew, M. Tabebordbar, J. K. W. Cheng, P. Mali, E. Y. Wu, A. H. M. Ng, K. Zhu, A. J. Wagers, G. M. Church, A multifunctional AAV-CRISPR-Cas9 and its host response. *Nat. Methods* **13**, 868–874 (2016).
53. C. T. Charlesworth, P. S. Deshpande, D. P. Dever, J. Camarena, V. T. Lemgart, M. K. Cromer, C. A. Vakulskas, M. A. Collingwood, L. Zhang, N. M. Bode, M. A. Behlke, B. Dejene, B. Cieniewicz, R. Romano, B. J. Lesch, N. Gomez-Ospina, S. Mantri, M. Pavel-Dinu, K. I. Weinberg, M. H. Porteus, Identification of preexisting adaptive immunity to Cas9 proteins in humans. *Nat. Med.* **25**, 249–254 (2019).
54. Y. Zhang, C. Long, R. Bassel-Duby, E. N. Olson, Myoediting: Toward prevention of muscular dystrophy by therapeutic genome editing. *Physiol. Rev.* **98**, 1205–1240 (2018).
55. H. Yin, F. Price, M. A. Rudnicki, Satellite cells and the muscle stem cell niche. *Physiol. Rev.* **93**, 23–67 (2013).
56. O. Bergmann, R. D. Bhardwaj, S. Bernard, S. Zdunek, F. Barnabé-Heider, S. Walsh, J. Zupicich, K. Alkass, B. A. Buchholz, H. Druid, S. Jovinge, J. Frisén, Evidence for cardiomyocyte renewal in humans. *Science* **324**, 98–102 (2009).
57. O. Bergmann, S. Zdunek, A. Felker, M. Salehpour, K. Alkass, S. Bernard, S. L. Sjostrom, M. Szewczykowska, T. Jackowska, C. Dos Remedios, T. Malm, M. Andrä, R. Jashari, J. R. Nyengaard, G. Possnert, S. Jovinge, H. Druid, J. Frisén, Dynamics of cell generation and turnover in the human heart. *Cell* **161**, 1566–1575 (2015).
58. S. Shen, K. D. Bryant, S. M. Brown, S. H. Randell, A. Asokan, Terminal *N*-linked galactose is the primary receptor for adeno-associated virus 9. *J. Biol. Chem.* **286**, 13532–13540 (2011).


**Acknowledgments:** We thank J. Cabrera for graphics; C. Wang and the Boston Children's Hospital Viral Core for AAV production; the Metabolic Phenotyping Core for serum CK analysis; the Sanger Sequencing Core and Next Generation Sequencing Core for sequencing service; the Flow Cytometry Core for cell sorting; V. Zaric and the Vector Core for quantitative PCR–based AAV titer analysis; B. Johnson and M. Bolukbasi for ddPCR-based AAV titer analysis; and N. Jones, A. Mcvie-Wylie, and L. Amoasii for constructive advice. We are grateful to S. Hauschka (University of Washington) for providing the muscle-specific CK8e promoter, D. Grimm (Heidelberg University Hospital, Germany) for providing the TRISPR-sgRNA expression plasmid, and S. Gray (University of Texas Southwestern Medical Center) for providing the scAAV plasmid. **Funding:** This work was supported by funds from NIH (HL130253 and AR-067294), the Senator Paul D. Wellstone Muscular Dystrophy Cooperative Research Center (U54 HD 087351), Exonics Therapeutics, and the Robert A. Welch Foundation (grant 1-0025 to E.N.O.). **Author contributions:** Y.Z., R.B.-D., and E.N.O. wrote and edited the manuscript. Y.Z. designed the experiments; cloned AAV constructs; and performed the animal studies, tissue cryosectioning, imaging, and data analysis. H.L. performed the in vitro AAV transduction, genomic PCR, RT-PCR, deep sequencing library preparation, viral genome copy number detection, and data analysis. Y.-L.M. generated the ΔEx44 dystrophic mouse model and targeting strategy for exon 45 and performed AAV injection. E.S.-O. performed Western blot, immunohistochemistry, and imaging. J.H. performed the muscle electrophysiology analysis. A.A.M. performed the tissue processing experiments. J.M.S. performed immunohistochemistry and H&E staining. P.P.A.M. provided oversight of the electrophysiology analysis. J.K. analyzed deep sequencing data. **Competing interests:** Y.Z., R.B.-D., and E.N.O. are inventors on a provisional patent application related to this work filed by USPTO (no. 62/956,726., filed 3 January 2020). The authors declare no other competing interests. **Data and materials availability:** All data needed to evaluate the conclusions in the paper are present in the paper and/or the Supplementary Materials. Additional data related to this paper may be requested from the authors.

Submitted 9 July 2019
Accepted 3 December 2019
Published 19 February 2020
10.1126/sciadv.aay6812

**Citation:** Y. Zhang, H. Li, Y.-L. Min, E. Sanchez-Ortiz, J. Huang, A. A. Mireault, J. M. Shelton, J. Kim, P. P. A. Mammen, R. Bassel-Duby, E. N. Olson, Enhanced CRISPR-Cas9 correction of Duchenne muscular dystrophy in mice by a self-complementary AAV delivery system. *Sci. Adv.* **6**, eaay6812 (2020).